

# Nanosecond molecular relaxations in lipid bilayers studied by high energy resolution neutron scattering and in-situ diffraction

Maikel C. Rheinstädter<sup>1,\*</sup>, Tilo Seydel<sup>1</sup>, and Tim Salditt<sup>2</sup>

<sup>1</sup>*Institut Laue-Langevin, 6 rue Jules Horowitz, BP 156, 38042 Grenoble Cedex 9, France*

<sup>2</sup>*Institut für Röntgenphysik, Friedrich-Hund Platz 1, 37077 Göttingen, Germany*

(Dated: August 18, 2018)

We report a high energy-resolution neutron backscattering study to investigate slow motions on nanosecond time scales in highly oriented solid supported phospholipid bilayers of the model system DMPC-d54 (deuterated 1,2-dimyristoyl-sn-glycero-3-phosphatidylcholine), hydrated with heavy water. Wave vector resolved quasi-elastic neutron scattering (QENS) is used to determine relaxation times  $\tau$ , which can be associated with different molecular components, i.e., the lipid acyl chains and the interstitial water molecules in the different phases of the model membrane system. The inelastic data are complemented both by energy resolved and energy integrated in-situ diffraction. From a combined analysis of the inelastic data in the energy and time domain, the respective character of the relaxation, i.e., the exponent of the exponential decay is also determined. From this analysis we quantify two relaxation processes. We associate the fast relaxation with translational diffusion of lipid and water molecules while the slow process likely stems from collective dynamics.

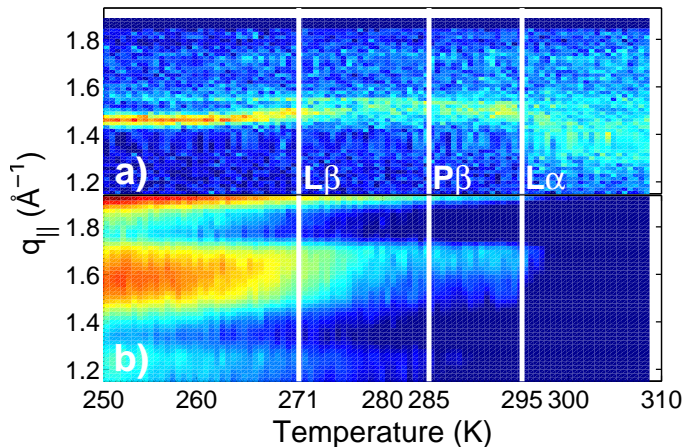
PACS numbers: 87.14.Cc, 87.16.Dg, 83.85.Hf, 83.10.Mj

## INTRODUCTION

Inelastic scattering techniques give a wave vector resolved access to dynamical properties, i.e., excitation frequencies or relaxation rates can be quantified at different internal length scales. This is important to associate the dynamics with individual modes of motion. A unique advantage lies in the simultaneous access to both structural and dynamical properties by measuring the scattering  $S(\vec{Q}, \omega)$  as a function of wave vector transfer  $\vec{Q}$  and energy transfer  $\omega$ . We hereby report on  $\mu\text{eV}$  energy resolved spectra in the model membrane system DMPC-d54, achieved by the neutron backscattering technique. By analyzing the respective  $Q$  dependence, we simultaneously probe low energetic density fluctuations of lipid acyl chains and interstitial water molecules, i.e., the water layer in between the stacked membranes.

The spectrum of fluctuations in biomimetic and biological membranes covers a large range of time and length scales [1, 2, 3, 4, 5, 6, 7, 8, 9], ranging from the long wavelength undulation and bending modes of the bilayer with typical relaxation times of nanoseconds and lateral length scales of several hundred lipid molecules to the short wavelength density fluctuations in the picosecond range on nearest neighbor distances of lipid molecules. Local dynamics in lipid bilayers, i.e., dynamics of individual lipid molecules as vibration, rotation, libration (hindered rotation) and diffusion, has been investigated by, e.g., incoherent neutron scattering [1, 2, 3, 4, 5] and nuclear magnetic resonance [10, 11] to determine the short wavelength translational and rotational diffusion constant. Collective undulation modes have been investigated using neutron spin-echo spectrometers [4, 5, 12, 13] and dynamical light scattering [14, 15, 16]. Only recently, the first inelastic scattering experiments in phospholipid

bilayers to determine collective motions of the lipid acyl chains and in particular the short wavelength dispersion relation have been performed using inelastic x-ray [17] and neutron [18] scattering techniques. While here fast propagating sound modes in the picosecond time range have been quantified, the present paper deals with slow nanosecond relaxation times on length scales of nearest neighbor distances of phospholipid acyl chains and water molecules, i.e., the slow dynamics of melting (diffusion) and collective movements (most likely undulations) of the lipid and water backbone. We have selected the neutron backscattering technique for this study since the dynamical modes at high  $q_{||}$  (the in plane component of the scattering vector  $\vec{Q}$ ) are too fast to be accessed by x-ray photon correlation spectroscopy (XPCS) and the lateral length scales are too small to be resolved by dynamic light scattering (DLS) or neutron spin-echo technique (NSE). Note that the feasibility of wave vector resolved backscattering experiments in oriented membrane systems to study freezing of lipid acyl chains and water molecules has been established only recently [19]. In this work we present the unprecedented determination of relaxation rates from  $Q$ -resolved backscattering QENS data in phospholipid bilayers, combined with in-situ diffraction to unambiguously assign the relaxation times to the respective phases of the model membranes. These measurements are carried out in aligned phases to preserve the unique identification of modes on the basis of the parallel and perpendicular components  $q_{||}$ , the lateral momentum transfer in the plane of the bilayers, and  $q_z$ , the reflectivity, of the scattering vector  $\vec{Q}$ .



## EXPERIMENTAL

In the case of single membranes the inelastic neutron scattering signal is by far not sufficient for a quantitative study of the inelastic scattering. Partially (acyl chain) deuterated DMPC-d54 (1,2-dimyristoyl-sn-glycero-3-phosphatidylcholine) was obtained from Avanti Polar Lipids. Highly oriented multi lamellar membrane stacks of several thousands of lipid bilayers were prepared by spreading lipid solution of typically 25mg/ml lipid in trifluoroethylene/chloroform (1:1) on 2" silicon wafers, followed by subsequent drying in vacuum and hydration from D<sub>2</sub>O vapor [20], resulting in a structure of smectic A symmetry. Twenty such wafers separated by small air gaps were combined and aligned with respect to each other to create a "sandwich sample" consisting of several thousands of highly oriented lipid bilayers (total mosaicity about 0.5°), with a total mass of about 400 mg of deuterated DMPC. The sample was mounted in a hermetically sealed aluminium container within a cryostat and hydrated from D<sub>2</sub>O vapor. Saturation of the vapor in the voids around the lipids was assured by placing a piece of pulp soaked in D<sub>2</sub>O within the sealed sample container. The pulp was shielded by Cadmium to exclude any parasitic contribution to the scattering. The hydration was not controlled but we allowed the sample to equilibrate for 10 h at room temperature before the measurements. The large beam divergence as compared to reflectometers did not allow to determine the corresponding  $d_z$  spacing simultaneously with sufficient accuracy to, e.g., determine the swelling state of the membrane stack. We note that the absolute level of hydration is therefore not precisely known but the temperature of the main transition agrees quite well with literature values.

The experiment was carried out at the cold neutron backscattering spectrometer IN16 [21] at the Institut Laue-Langevin (ILL) in its standard setup with Si(111) monochromator and analyzer crystals corresponding to an incident and analyzed neutron energy of 2.08 meV

FIG. 1: (Color online). (a) Energy integrated diffraction for temperatures 250 K < T < 310 K with a temperature resolution of  $\Delta T \approx 0.3$  K (normalized to acquisition time).  $q_{||}$  is the in-plane component of the scattering vector  $\vec{Q}$ . The phase boundaries for gel (L $\beta$ ), ripple (P $\beta'$ ) and fluid phase (L $\alpha$ ) as defined by structural changes, i.e., the change of peak position and width are marked by the solid white lines. (b) 'True' elastic scattering, measured with an energy resolution of 0.9  $\mu$ eV. The phase transitions are also visible in the energy resolved diffraction data by following the melting at the lipid acyl chain and water position. Data are normalized to monitor, detector efficiency normalized to the scattering signal of a 2 mm thick Vanadium plate oriented at 135° with respect to the incoming beam. Please note that no absorption correction has been done. For geometrical reasons the diffraction detectors have a lower maximum  $q_{||}$  than the backscattering detectors.

( $\lambda=6.27$  Å) resulting in a high resolution in energy transfer of about 0.9  $\mu$ eV FWHM. An energy transfer of  $-15\mu\text{eV} < E < +15\mu\text{eV}$  can be scanned by varying the incident energy by Doppler-shifting the incident neutron energy through an adequate movement of the monochromator crystal. 20 detectors in exact backscattering with respect to the analyzer crystals covering an angular width of 6.5° each have been used. Note that the maximum of the static *bulk* water correlation peak at about  $q_{||} \approx 2$  Å<sup>-1</sup> is not accessible because of simple geometrical reasons. The set-up is therefore more sensitive to detect *amorphous* water with slightly larger nearest neighbor distances, as it is expected to occur in the water layers of the stacked bilayers. A separate line of 160 energy integrating diffraction detectors – normally mounted on a parallel circle inclined by 24.4° below the scattering plane – with an angular width of 1° each – allows to simultaneously detect structural changes with a much higher  $q_{||}$  resolution.

## RESULTS FROM NEUTRON DIFFRACTION

We thus simultaneously performed two types of diffraction measurements, namely energy-resolved and energy-integrated measurements. Note that the additional diffraction detectors very well integrate over low lying excitations and relaxations. Figure 1 (a) shows an energy integrated diffraction pattern for  $1.1 \text{ Å}^{-1} < q_{||} < 1.85 \text{ Å}^{-1}$ . From the temperature dependence of the inter-acyl chain correlation peak at  $q_{||} \approx 1.4 \text{ Å}^{-1}$  we assign the transition temperatures of gel to ripple phase (L $\beta$ -P $\beta'$ ) to 285 K and the temperature of the main transition (P $\beta'$ -L $\alpha$ ) to T=295 K. T<sub>fw</sub>=271 K marks the freezing temperature of the amorphous water layer in between the stacked membranes [19]. The correlation peak gradually shifts to smaller  $q_{||}$  values below T<sub>fw</sub> until about 264 K. In the range 264 K < T < 271 K water migrates out the bilayer stacks to freeze as bulk water, as discussed in detail in

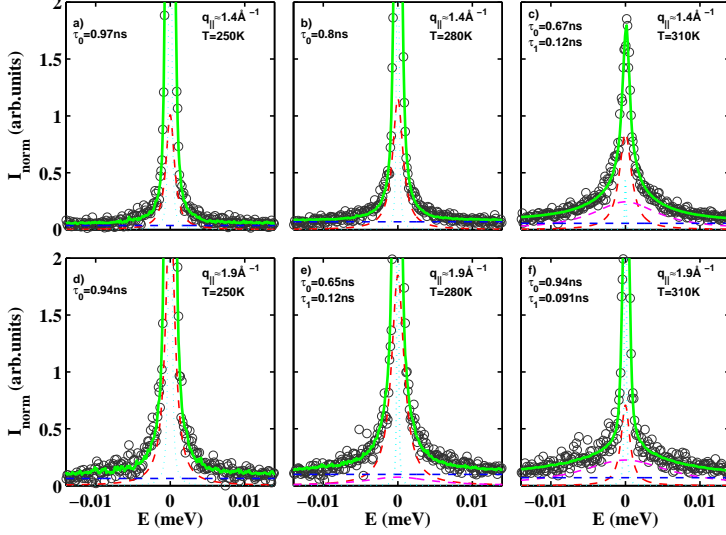


FIG. 2: (Color online). Inelastic scans at the lipid chain ( $q_{||} \approx 1.4 \text{ \AA}^{-1}$ ) and water ( $q_{||} \approx 1.9 \text{ \AA}^{-1}$ ) position for temperatures  $T=250 \text{ K}$ ,  $280 \text{ K}$  and  $310 \text{ K}$ . Detectors have been grouped to increase counting statistics. The inter acyl chain correlation peak is measured by detectors 9-13, which cover a  $q_{||}$  range of  $1.20 \text{ \AA}^{-1} < q_{||} < 1.60 \text{ \AA}^{-1}$ . The water contribution is detected by detectors 17-20 covering  $1.78 \text{ \AA}^{-1} < q_{||} < 1.94 \text{ \AA}^{-1}$ . As a model, up to two Lorentzian peak profiles (dashed lines) to describe the quasi elastic broadening and a Dirac function (dotted line) to describe the elastic intensity were assumed. This model was convoluted with the measured resolution function obtained from a Vanadium standard. A flat background (dashed line) was subsequently added and the result was fitted (fit result: solid line) to the data (circles). A flat background may arise from fast processes far beyond the accessible energy window of the spectrometer. The thus obtained relaxation times are given in the figures. The calibration error of the energy scale is approx. 3%.

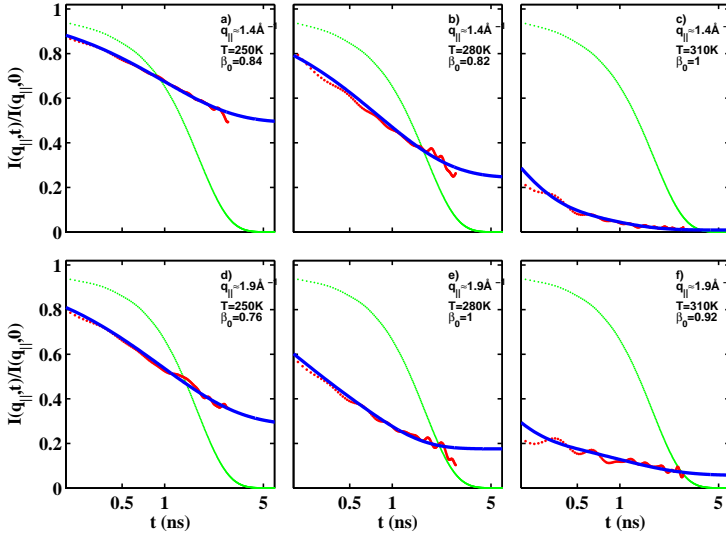


FIG. 3: (Color online). Corresponding Fourier transformed energy space data (power spectra) from Fig. 2 (points), divided by an analytical description of the Vanadium resolution. The thus obtained intermediate scattering function  $I(q_{||}, t)/I(q_{||}, 0)$  is shown together with the fits (blue solid line) of two exponential decays  $I(q_{||}, t)/I(q_{||}, 0) = (A_0 - A_1) \exp[-(t/\tau_0(q_{||}))^{\beta_0}] + y_1 + (A_1 - y_1) \exp[-(t/\tau_1(q_{||}))^{\beta_1}]$ . The values for  $\tau_{0,1}$  have been fixed from the energy scans and only the exponents  $\beta_{0,1}$  and the amplitudes  $A_{0,1}$  have been fitted. The thus obtained values for  $\beta_0$  are given in the figures. The resolution is also plotted (green line). While the data at  $250 \text{ K}$  are well described by one exponential decay, two decays are needed at higher temperatures.

Ref. [19]. The energy resolved pattern in Fig. 1 (b) sheds light on the melting process of lipid acyl chains and water and perfectly reproduces the results previously reported in [19] (the difference being the larger number of detectors). Only structures which are static with respect to the energy resolution of  $0.9 \text{ \mu eV}$ , which correspond to motions slower than approx.  $4 \text{ ns}$ , are detected as elastic when using the energy resolving backscattering detectors. Changes in this intensity may arise from either structural or dynamical changes, i.e., shifts of correlation peaks or freezing or melting of dynamical modes. Elastic intensity at the water detectors rises at  $T < 271 \text{ K}$ ; at the acyl chain position there is an elastic contribution below  $295 \text{ K}$ , the temperature of the main transition. A further increase occurs when entering the gel ( $L\beta$ ) phase indicating the high degree of dynamics in the ripple ( $P\beta'$ ) phase. Note that there is very little elastic contribution in the fluid phases pointing out that the intensity usually measured

in diffraction experiments stems predominantly from low lying fluid excitations and quasi elastic scattering.

## INELASTIC SCATTERING

Based on the diffraction patterns we have recorded inelastic scans at temperatures of  $T=250 \text{ K}$ ,  $280 \text{ K}$ ,  $292 \text{ K}$  and at  $310 \text{ K}$ , far in the fluid  $L\alpha$  phase of the model membranes. Additional scans in the regime of critical swelling ( $T=296, 297, 299$  and  $303 \text{ K}$ ) have also been taken. The results for the acyl chain ( $q_{||} \approx 1.4 \text{ \AA}^{-1}$ ) and the water position ( $q_{||} \approx 1.9 \text{ \AA}^{-1}$ ) are depicted in Fig. 2. At  $250 \text{ K}$ , both  $q_{||}$  positions are well fitted by a single Lorentzian, i.e., a single relaxation process with an energy width (FWHM)  $\Delta\omega$  and corresponding relaxation time  $\tau = 2\pi/\Delta\omega$ . For temperatures above  $280 \text{ K}$  for the water and above  $292 \text{ K}$  for the acyl chains two

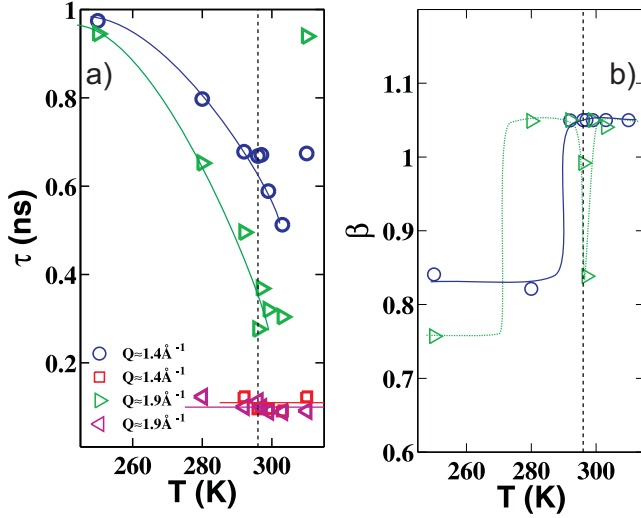


FIG. 4: (Color online). (a) Relaxation times at the lipid chain and the water position for all measured temperatures as determined from fits to the quasi elastic data in Fig. 2. (b) Exponents of the exponential decay as determined from fits of the intermediate scattering function from Fig. 3. Solid lines are guides to the eye.

Lorentzians are needed to describe the data. Although the Lorentzians describe the energy spectra, small deviations from the fits are visible pointing to deviations from single exponential relaxations. A detailed analysis in energy space is difficult and would mean to add more Lorentzian or mix Lorentzian and Gaussian peak profiles with the risk of being physically meaningless. To further characterize the relaxation processes the data have been Fourier transformed (using the Matlab FFT algorithm) to determine the exponent  $\beta$  of the corresponding exponential decays in time domain,  $\exp[-(t/\tau)^\beta]$ , from fits to the intermediate scattering function  $I(q_{||}, t)$ , as shown in Fig. 3. With increasing temperature there is a relaxation step moving into the time window at the two  $q_{||}$  positions, respectively. Because of the limited dynamical range of  $15\text{ }\mu\text{eV}$ , the shortest time accessible is about 0.2 ns and the faster process is already partially out of the accessible time window, i.e., the quasielastic broadening is slightly broader than the energy window. No exponent could therefore be reliably determined for the fast process. The resulting relaxation times  $\tau_{0,1}$  and the corresponding exponent of the slow process,  $\beta_0$ , are depicted in Fig. 4 (a) and (b) for all measured temperatures. To gain reliable fitting parameters for  $\tau$  and  $\beta$ , the relaxation times  $\tau_{0,1}$  have been determined from the energy spectra  $S(q_{||}, \omega)$  in Fig. 2 because this gives the highest accuracy and stability. The  $\tau$  values have then been fixed for the fits of the exponential decay in the time domain.  $\beta$  is determined from the fits to  $I(q_{||}, t)$  in Fig. 3. The two processes at the two  $q_{||}$  positions show distinctly different relaxation times and temperature dependencies.

While the fast process has constant times of about 0.1 ns, the slow process starts at about 1 ns at 250 K and becomes faster as approaching the main phase transition at 295 K. Note that because of the limited dynamical range the accuracy in determining the fast relaxation time  $\tau_1$  is also limited and we can not exclude a temperature dependence of the fast process. While for the fast branches no exponent can be determined for the same reason, the slow processes show a stretched exponential character at low temperatures and turn to single exponential when the corresponding correlations melt at the lipid (main transition) and water melting temperature, respectively.

## DISCUSSION

From the inelastic neutron data we quantify two relaxation times. We argue that the corresponding processes stem from collective motions of the lipid acyl chains and interstitial water molecules, respectively, rather than from local dynamics. By selective deuteration of the chains and hydration from  $\text{D}_2\text{O}$  vapor, coherent motions are strongly enhanced over other contributions to the inelastic scattering cross section [23]. The fast process  $\tau_1$  disappears below the freezing temperature of the lipids ( $P\beta'$  phase) respective water molecules ( $T < T_{fw} = 271\text{ K}$ ) and might therefore be due to (collective) translational diffusion of lipids and water. The slow process with relaxation times  $\tau_0$  is measured down to the lowest temperatures of  $T = 250\text{ K}$  and most likely probes collective dynamics, i.e., neighboring lipid and water molecules participating in slow mesoscopic dynamics. However, to further characterize this process,  $q_{||}$  dependent data are needed to determine the corresponding dispersion relation and compare to theoretical models. It is speculated in the literature that the minimum in the dispersion relation of the collective fast propagating modes at the nearest neighbor distances of lipid acyl chains (as determined in Refs. [17] and [18]) is related to transport phenomena within and across the bilayers. The relaxation found in the present paper on the same length but distinctly different time scale might be relevant to establish such a model of *phonon assisted diffusion* in membranes, which would be of particular interest in membrane biophysics and biotechnology applications.

The slow relaxations at the acyl chain and the water position both show a decrease of relaxation times towards the main transition of the phospholipids. The relaxation time of the fast branch with  $\tau \approx 0.1\text{ ns}$  that we attribute to translational diffusion is temperature independent within the experimental accuracy, which is slightly limited by the maximum achievable energy transfer. Note that the diffusion time measured here can be interpreted as time for hopping processes to nearest neighbor sites. Such a process needs a free neighboring site but does not necessarily give information about the mobility



of these *holes* (free surface or volume) what would be important for macroscopic diffusion. The corresponding time scales and diffusion constants might therefore be distinctly different. From measurements with a higher dynamical range, the energy barrier of this excitation could probably be determined from the temperature dependent hopping times using Arrhenius or Vogel-Fulcher laws.

The  $\beta$  exponents in Fig. 4 (b) start at values  $\beta < 1$  at low temperatures. Structural inhomogeneities and heterogeneous interactions obviously lead to a local relaxation dynamics and to stretched ( $\beta < 1$ ) exponentials. When entering the fluid phase at  $T_m$ , the lipid relaxations ( $q_{||} \approx 1.4 \text{ \AA}^{-1}$ ) turn into single exponential, as can be expected for a diffusive, fluid like motion of the particles. At the water position ( $q_{||} \approx 1.9 \text{ \AA}^{-1}$ ), the transition from stretched to single exponential occurs between 250 K and 280 K, most likely at the water freezing or melting temperature  $T_{fw}=271 \text{ K}$ , as speculated and indicated in the Figure. A striking feature is that in the range of critical swelling, the water relaxations become again stretched what might be related to the expansion of the water layer leading to the well known anomalous swelling of phospholipid bilayers close to the main transition [22].

## CONCLUSION

In conclusion, using the neutron backscattering technique, we have determined  $q_{||}$ -dependent relaxation times at different temperatures in the model membrane system DMPC that we attribute to lipid acyl chains and interstitial water molecules. In-situ diffraction allowed to clearly assign the temperatures to the different phases of the bilayers. A combined data analysis in the energy and time domain allowed to quantify relaxation times of two processes and determine the exponents  $\beta$  of the exponential decays. The fast process is attributed to diffusion while the slow process likely stems from collective dynamics. We find stretched exponential relaxations at low temperatures. The relaxations turn into single exponential above the corresponding melting temperatures of lipid and water molecules.

Future experiments, which will include a selective deuteration of the acyl-chains and the membrane water, respectively, will allow to mask different types of mobility and hopefully deduce complete dispersion relations of the different molecular components in the different phases of the phospholipid bilayers. Compared to NSE and XPCS, large  $Q$ -values can easily be obtained. The current drawback of the technique is the limited dynamical range on high-flux spectrometers which hopefully will be overcome in next generation neutron sources and backscattering spectrometers. Our study also points to the wealth of new information that can be explored with the membrane

backscattering technique.

**Acknowledgement:** We acknowledge T. Gronemann (Institut für Röntgenphysik, Göttingen) for help with the sample preparation and M. Elender (ILL) for technical and engineering support and the ILL for the allocation of beam time.

---

\* Electronic address: rheinstaedter@ill.fr

- [1] S. König, W. Pfeiffer, T. Bayerl, D. Richter, and E. Sackmann, *J. Phys. II France* **2**, 1589 (1992).
- [2] S. König, E. Sackmann, D. Richter, R. Zorn, C. Carlile, and T. Bayerl, *J. Chem. Phys.* **100**, 3307 (1994).
- [3] S. König, T. Bayerl, G. Coddens, D. Richter, and E. Sackmann, *Biophys. J.* **68**, 1871 (1995).
- [4] W. Pfeiffer, T. Henkel, E. Sackmann, and W. Knorr, *Europhys. Lett.* **8**, 201 (1989).
- [5] W. Pfeiffer, S. König, J. Legrand, T. Bayerl, D. Richter, and E. Sackmann, *Europhys. Lett.* **23**, 457 (1993).
- [6] E. Lindahl and O. Edholm, *Biophys. J.* **79**, 426 (2000).
- [7] R. Lipowsky and E. Sackmann, eds., *Structure and Dynamics of Membranes*, vol. 1 of *Handbook of Biological Physics* (Elsevier, Amsterdam, 1995).
- [8] T. Bayerl, *Curr. Opin. Colloid Interface Sci.* **5**, 232 (2000).
- [9] T. Salditt, *Curr. Opin. Colloid Interface Sci.* **5**, 19 (2000).
- [10] A. Nevzorov and M. Brown, *J. Chem. Phys.* **107**, 10288 (1997).
- [11] M. Bloom and T. Bayerl, *Can. J. Phys.* **73**, 687 (1995).
- [12] T. Takeda, Y. Kawabata, H. Seto, S. Komura, S. Gosh, M. Nagao, and D. Okuhara, *J. Phys. Chem. Solids* **60**, 1375 (1999).
- [13] M. C. Rheinstädter, W. Häussler, and T. Salditt, accepted for publication (2006), cond-mat/0606114.
- [14] R. Hirn, T. Bayerl, J. Rädler, and E. Sackmann, *Faraday Discuss.* **111**, 17 (1998).
- [15] R. B. Hirn and T. M. Bayerl, *Phys. Rev. E* **59**, 5987 (1999).
- [16] M. F. Hildenbrand and T. M. Bayerl, *Biophys. J.* **88**, 3360 (2005).
- [17] S. Chen, C. Liao, H. Huang, T. Weiss, M. Bellissent-Funel, and F. Sette, *Phys. Rev. Lett.* **86**, 740 (2001).
- [18] M. C. Rheinstädter, C. Ollinger, G. Fragneto, F. Demmel, and T. Salditt, *Phys. Rev. Lett.* **93**, 108107 (2004).
- [19] M. C. Rheinstädter, T. Seydel, F. Demmel, and T. Salditt, *Phys. Rev. E* **71**, 061908 (2005).
- [20] C. Münster, T. Salditt, M. Vogel, R. Siebrecht, and J. Peisl, *Europhys. Lett.* **46**, 486 (1999).
- [21] B. Frick and M. Gonzalez, *Physica B* **301**, 8 (2001).
- [22] G. Pabst, J. Katsaras, V. A. Raghunathan, and M. Rapolt, *Langmuir* **19**, 1716 (2003).
- [23] Neutron scattering data may include contributions from coherent and incoherent scattering, i.e., from pair- and autocorrelated scattering (collective and local or diffusive modes). While in protonated samples the *incoherent* scattering is usually dominant and the time-autocorrelation function of individual scatterers is accessible in neutron scattering experiments, (partial) deuteration emphasizes the *coherent* scattering and gives access to collective motions by probing the pair correlation function.